JOURNAL OF CATALYSIS 138, 630–639 (1992)

Structure of Mn–Zr Mixed Oxide Catalysts and Their Catalytic Properties in the CO Hydrogenation Reaction

DONG JUN KOH, JONG SHIK CHUNG,[1] YOUNG GUL KIM, JAE SUNG LEE, IN-SIK NAM, AND SANG HEUP MOON*

*Department of Chemical Engineering, Pohang Institute of Science & Technology (POSTECH) & Research Institute of Science and Technology (RIST), P.O. Box 125, Pohang 790-600, Korea, and *Department of Chemical Engineering, Seoul National University, Seoul 151-742, Korea*

Received July 24, 1991; revised June 4, 1992

Mn–Zr oxide catalysts with varying Mn–Zr ratio were prepared by a coprecipitation method. Their structure and catalytic properties were studied by means of N_2 adsorption, XRD, TPR, and CO hydrogenation as a probe reaction. The precipitated Mn–Zr mixed oxide was composed of a mixture of large particles of manganese oxide and small particles of zirconium oxide. Addition of Mn retarded the growth of fine particles of zirconium oxide. By calcination at high temperature, part of the manganese oxide forms a solid solution with zirconium oxide and deposits on the surface of zirconium oxide as a thin layer. The type of Mn present in the mixed oxide affected the selectivity pattern in the CO hydrogenation. The bulk Mn exhibited a high selectivity to isobutene, but products contained hydrocarbons higher than C_5. Mn dispersed on the surface of zirconium oxide showed a similar selectivity pattern to bulk Mn, but hydrocarbon chain growth was limited to C_4 or lower. The formation of a solid solution enhanced production of lower hydrocarbons, especially methane.

INTRODUCTION

Zirconium oxide is known to enhance the production of alcohols when it is used as a catalyst support in the CO hydrogenation reaction. For example, zirconium oxide-supported Cu catalyst exhibits both high activity and selectivity toward methanol systhesis (*1, 2*). Rh impregnated on zirconium oxide favors the formation of ethanol (*3*). Meanwhile, there are another reports that zirconium oxide itself can catalyze the CO hydrogenation reaction and produces isobutene very selectively at atmospheric pressure (*4, 5*). The reaction mechanism for the synthesis reaction over pure zirconium oxide has been extensively studied by the Ekerdt group (*6–10*). It has been proposed that methoxide formed through a formate-to-methoxide mechanism is responsible for the production of methanol and methane, and that two chain growth mechanisms, reaction of enolate forms of C_3 hydrocarbon with either methoxide or CO, account for the isosynthesis to produce branched hydrocarbons.

Studies of zirconium oxide mixed with another oxide as catalyst for the synthesis reaction can be found in a few cases. Yttria-doped zirconium oxide was tested in the CO hydrogenation reaction and oxygen anion vacancy on the zirconium oxide surface is known to be responsible for the formation of methanol (*10*). Recently the Keim group (*11, 12*) reported a catalyst system based on zirconium–manganese mixed oxide which produced isobutanol very selectively during the CO hydrogenation. The addition of a small amount of Pd to the Mn–Zr mixed oxide increased selectivity to isobutanol substantially: up to 44% at the reaction conditions of 420°C and 150–250 bar. However,

[1] To whom correspondence should be addressed.

0021-9517/92 $5.00

the structure and properties of the mixed oxide have not been reported in detail. During the study of manganese oxide in our laboratory, it was found that manganese oxide was as active as zirconium oxide in the CO hydrogenation reaction with a high yield of isobutene. This motivated us to study the catalytic role of manganese in the Mn–Zr mixed oxide.

In the present work, we studied the CO hydrogenation reaction over pure manganese oxide and a series of Mn–Zr mixed oxides having varying Mn content. The focus was on the study of the morphology and structure of the mixed oxide and correlation of these factors with catalytic activity and selectivity in the systhesis reaction.

EXPERIMENTAL

Catalyst Preparation

Catalysts were prepared by the precipitation method. Aqueous solutions having various ratios of Mn/Zr were prepared by dissolving zirconium oxynitrate (Alfa) and manganese nitrate (50% solution supplied from Alfa). 5 wt% ammonia solution was added to the solution of Mn and Zr ions with continuous stirring at 80°C until the solution pH became 8. The precipitate was filtered and washed with deionized and distilled water, and then dried at 120°C for 16 h. The prepared catalyst was designated, for example, as 20Mn/Zr, where the number represents Mn content (as wt%) in the Mn–Zr mixture. Pure Mn oxide and Zr oxide were also prepared by the same precipitation method. For comparison, an impregnated catalyst, 5Mn/Zr-IM, with Mn content of 5 wt% was prepared by impregnating zirconium oxide calcined at 500°C with an aqueous solution of Mn by the incipient wetness preparation method.

Catalyst Characterization

Catalysts were characterized by N_2 adsorption, X-ray diffraction (XRD), X-ray photoelectron spectroscopy (XPS), and temperature programmed reduction (TPR). The adsorption experiment was carried out using a gas adsorption analyzer made by Micromeritics (Model Accusorb 2100E). X-ray diffraction measurements were performed using a Rigaku DMAX-B diffractometer with Cu$K\alpha$ radiation. XPS measurements were carried out in a Perkin–Elmer Model PHI 5400 spectrometer using a catalyst wafer. IR spectra were recorded on a Perkin–Elmer Model 1800 Fourier-transform IR spectrometer. A spectrum was calculated after collecting 250 scans at 4 cm^{-1} resolution.

TPR spectra were obtained by measuring hydrogen consumption with a thermal conductivity detector. A gas mixture of 5% hydrogen in argon was passed at a flow rate of 40 ml/min through a bed containing 0.5 g of catalyst sample. The effluent gas was passed through a silica trap maintained at −97°C to remove water, then through the thermal conductivity detector. The sample was first oxidized at 500°C for 3 h in flowing oxygen, and then hydrogen consumption was monitored as the sample was heated from room temperature to 800°C at a rate of 10°C/min. For the repeated TPR measurement, the catalyst was reoxidized with oxygen at 500°C for 3 h after the previous TPR measurement and this was followed by the next TPR measurement.

Reaction Testing

Catalytic activity and selectivity for CO hydrogenation were tested using a fixed-bed reactor made of $\frac{3}{8}$-in. quartz tube. The reactor was charged with about 5 g of catalyst, which was pretreated in a flow of oxygen at 500°C for 3 h. Then, reaction gas mixture with H_2/CO ratio of 1.0 was passed through the reactor. Hydrogen gas was purified by passing through a bed of Pd/alumina and molecular sieve to remove oxygen and water, respectively. Carbon monoxide was passed through a bed of MnO/silica and molecular sieve. The reaction products were analyzed using a gas chromatograph (Hewlett Packard 5890) equipped with FID detector and Alltech RSL-160 capillary column. 1-Butene and isobutene in C_4 hydrocarbons

were separated by a 7 ft. long, $\frac{1}{8}$ in. diameter 0.19% picric acid on Graphpac-GC column. Conversion of CO to hydrocarbons was typically less than 2%.

RESULTS AND DISCUSSION

Characterization of Catalyst Structure

X-ray diffraction patterns for pure zirconium oxides are shown in Fig. 1. The samples calcined at low temperatures (200–300°C) showed very broad and ill-defined peaks. When the calcination temperature was raised to above 500°C, well-resolved and sharp peaks appeared. In conjunction with the peak sharpening, it was observed that there was a corresponding decrease in the BET surface area, from 290 m^2/g after calcination at 200°C to 65 m^2/g at 500°C. Therefore, the breadth in the X-ray peak was considered to be due to the small particle size of zirconium oxide. Analysis of the peaks for the sample calcined at 500°C confirmed that the catalyst consisted of mainly monoclinic phase with a small amount of tetragonal phase. Unlike zirconium oxide, the pure manganese precipitate, when dried in air at 120°C, yielded sharp and strong peaks in the X-ray diffraction pattern which corresponded to Mn_3O_4 crystal structure. Calcination at 500°C oxidized it to the crystalline form of Mn_2O_3. The X-ray diffraction pattern of Mn-rich mixed oxide, for example 95Mn/Zr, also showed only peaks of manganese oxide, and was the same as those of the pure manganese oxide.

Figure 2 shows X-ray diffraction patterns for various Mn/Zr mixed oxides after calcination at two different temperatures. For the mixed oxide with low Mn content, as in the case of 5Mn/Zr, both the low temperature (A) and the high temperature (A′) calcinations yielded X-ray diffraction peaks corresponding to only zirconium oxide. No peak of manganese oxide was detected, indicating that the particle size is very small.

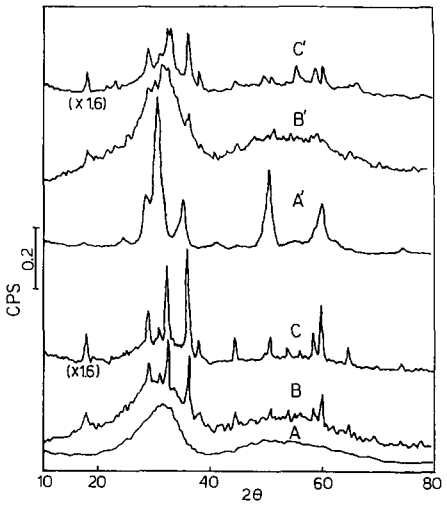

FIG. 2. X-ray diffraction patterns of Mn–Zr oxide catalysts after calcination. (A) 5Mn/Zr calcined at 120°C for 16 h; (B) 20Mn/Zr calcined at 120°C for 16 h; (C) 50Mn/Zr calcined at 120°C for 16 h; (A′) 5Mn/Zr calcined at 500°C for 3 h; (B′) 20Mn/Zr calcined at 500°C for 3 h; (C′) 50Mn/Zr calcined at 500°C for 3 h.

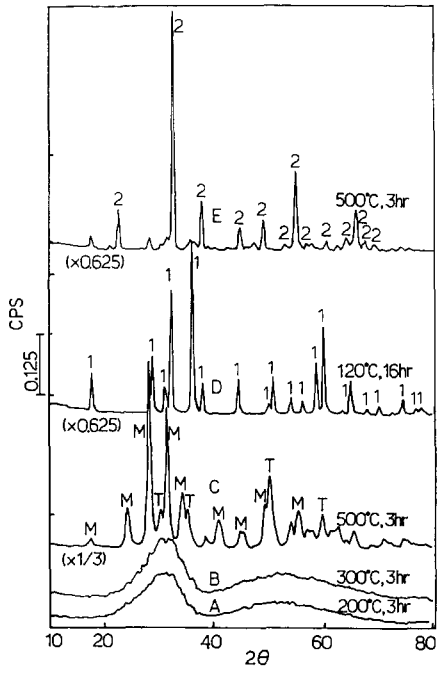

FIG. 1. X-ray diffraction patterns of pure manganese and zirconium oxide catalysts at various pretreatment conditions (M: monoclinic phase; T: tetragonal phase; 1: Mn_3O_4 phase; 2: Mn_2O_3 phase). (A–C) Zr; (D, E) Mn.

The sharp peaks of zirconium oxide obtained after calcination at 500°C (A′) corresponded to the crystalline form of tetragonal structure. Normally, pure zirconium oxide has a monoclinic structure at room temperature and transforms to the tetragonal structure at 1170°C (*13*). Our results in Fig. 1 also confirmed that pure zirconium oxide calcined at 500°C had the monoclinic structure. However, it is known that Y_2O_3 (*14*) or PbO (*15*) doped zirconium oxide can be stabilized in the tetragonal form at low temperature by the formation of a solid solution. Therefore the formation of the tetragonal phase in the 5Mn/Zr supports the hypothesis that manganese oxide is consumed in the formation of the solid solution by direct substitution of Mn cation for the host lattice Zr cation.

For the mixed oxides with manganese content in the intermediate range, as in the cases of 20Mn/Zr and 50Mn/Zr, both manganese oxide and zirconium oxide phases could be detected by the X-ray analysis. When these samples were dried at 120°C (B and C in Fig. 2), it was observed that sharp peaks of Mn_3O_4 phase were overlapped with broad and ill-defined peaks of zirconium oxide phase. This indicates that coprecipitation of the two components yields an oxide mixture in which relatively large particles of manganese oxide are mixed with small grains or crystallites of zirconium oxide. When the calcination temperature was increased to 500°C (B′ and C′ in Fig. 2), several changes in the X-ray diffraction patterns were noticed. First of all, the peak intensity of the manganese oxide phase decreased substantially compared with those obtained after drying at 120°C (B and C in Fig. 2). This indicates that the high temperature calcination induces a strong interaction between manganese oxide and zirconium oxide particles so that a large portion of manganese oxide particles is either dispersed on the surface of zirconium oxide or consumed in the formation of a solid solution with zirconium oxide. The structural modification of manganese oxide phase can also be supported by the difficulty in the oxidation of manganese oxide. Analysis of the weakened peaks of the manganese phase (B′ and C′ in Fig. 2) shows that manganese oxide is composed of a mixture of Mn_3O_4 and Mn_2O_3. The result is different from the complete oxidation of pure manganese oxide to Mn_2O_3. Second, as compared with the sharp peaks of zirconium oxide phase in the 5Mn/Zr (A′), the peaks of zirconium oxide phase in either 20Mn/Zr (B′) or 50Mn/Zr (C′) remained broad and ill-defined even after the high temperature calcination. This result confirms that zirconium oxide particles can be prevented from sintering and that crystallite growth is retarded by the incorporation of Mn.

TABLE 1

Atomic Concentration Ratios of Mn and Zr for Mn–Zr Mixed Oxides Calcined at 500°C for 3 hr

Catalyst	Composition (Mn : Zr)	
	Fresh	After Ar ion sputtering
50Mn/Zr	57.7 : 42.3	63.1 : 26.9
20Mn/Zr	30.1 : 69.9	33.3 : 66.7
5Mn/Zr	6.6 : 93.4	5.5 : 94.5
5Mn/Zr-IM	10.2 : 89.8	7.4 : 92.6

XPS spectra for the mixed oxides were recorded after calcination at 500°C. Table 1 shows the relative concentrations of Mn and Zr, both before and after Ar ion sputtering. In the cases of 20Mn/Zr and 50Mn/Zr, Mn concentrations increase after the Ar sputtering. However, the Mn concentration of 5Mn/Zr decreases after sputtering. This may indicate that manganese oxide in 5Mn/Zr is doped on the zirconium oxide particles. However, it does not imply that manganese is highly dispersed on the surface of zirconium oxide. Moreover, we could not find any noticeable shift in the binding energy of Mn peaks for various Mn/Zr mixed oxides. The Mn $2P_{3/2}$ peaks for all the samples were within 641.4 ± 0.4 eV. It must also be remembered that the sample is a pressed powder, so that it is not easy to speculate on the

TABLE 2

The BET Surface Area, Pore Volume, and Average Pore Size of Pure and Mixed Oxides of Mn and Zr

Catalyst	Calcination temp. (°C)	Pore volume (cm^3/g)	Avg. pore size (Å)	BET area (m^2/g)
Zr	200	0.175	18	290
Zr	400	0.154	22	105
Zr	500	0.131	30	65
Mn	120	—	—	7.9
Mn	500	—	—	7.7
5Mn/Zr-IM	500	0.145	22	62
5Mn/Zr	500	0.272	40	95
20Mn/Zr	500	0.154	16	194
50Mn/Zr	500	—	—	149
95Mn/Zr	500	—	—	16

real structure or morphology of Mn/Zr oxide from the XPS results.

Table 2 shows nitrogen adsorption results on several oxides of Mn and Zr. The surface area of pure manganese oxide is one order of magnitude lower than that of zirconium oxide. Manganese is softer than zirconium and the result in Fig. 1 shows that large particles of Mn_3O_4 can be formed even after the low temperature oxidation at 120°C. Zirconium oxide is a hard refractory material and its particle size remains small when the calcination temperature is kept low. However, it is gradually sintered to form a finite crystallite size with an increase in the calcination temperature. The surface area of the mixed oxide is higher than that of pure zirconium oxide, except for manganese rich 95Mn/Zr, and becomes a maximum when the Mn content becomes 20%. The increase in the surface area was observed only when the mixed oxide was prepared by the coprecipitation method. When manganese oxide was doped on zirconium oxide which was precalcined at 500°C, the surface area and pore structure were similar to the original pure zirconium oxide as shown in the case of 5Mn/Zr-IM in Table 2.

In the case of the coprecipitated Mn/Zr mixed oxide, calcining the precipitate at low temperature causes the soft Mn phase to grow in size and form a separate phase of manganese oxide particles. Thus, the mixed oxide, after drying at 120°C, is composed of a mixture of two phases in which large particles of Mn oxide are randomly mixed with small particles of Zr oxide. This was shown in the X-ray diffraction patterns (B and C in Fig. 2). Therefore, relatively large particles of Mn_3O_4 are surrounded by small particles of zirconium oxide. This retards the crystallite growth of zirconium oxide since the chance of intimate contact among zirconium oxide particles is reduced. The addition of Mn also changed the pore structure of the mixed oxide; both pore volume and average pore size showed a maximum at Mn content of 5%.

Temperature Programmed Reduction and IR Spectra

Figure 3 illustrates TPR curves for some oxide samples of Mn and Zr which were calcined at 500°C for 3 h. Pure zirconium oxide (Fig. 3A) exhibited two peaks at temperatures around 420 and 640°C. The amount of hydrogen consumed for the two peaks was relatively small: 2.2×10^{-5} mol/g cat at 420°C and 2.8×10^{-5} mol/g cat at 640°C. This suggests that zirconium oxide is reduced only at surface layers. It is known that zirconium oxide has two different surface hydroxyl groups; i.e., bridged and terminal (*16*). We attribute the two TPR peaks to the reductions of these two hydroxyl groups. A TPR profile of pure manganese

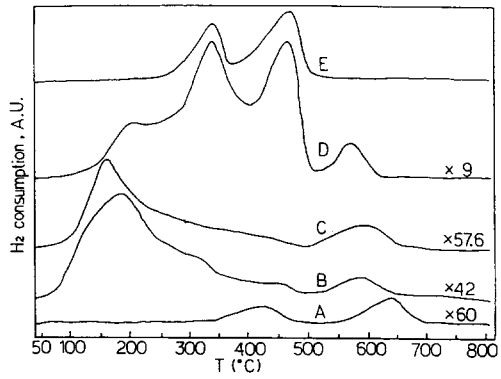

FIG. 3. TPR profiles of catalysts after oxidation at 500°C. (A) Zr, (B) 5Mn/Zr-IM, (C) 5Mn/Zr, (D) 20Mn/Zr, (E) Mn.

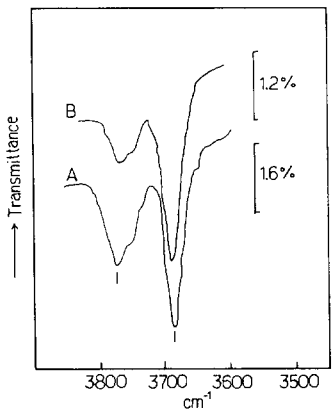

FIG. 4. IR spectra of catalysts after oxidation at 500°C followed by evacuation at 200°C. (A) Zr, (B) 5Mn/Zr.

oxide (Fig. 3E) also showed two peaks of hydrogen consumption. The peak at 340°C was ascribed to the reduction of Mn_2O_3 to Mn_3O_4 and the peak at 470°C to the reduction of Mn_3O_4 to MnO since the X-ray diffraction analysis taken at 360°C after the TPR experiment showed the reduced Mn oxide to be Mn_3O_4 and that at 500°C showed it to be MnO.

5Mn/Zr-IM, Mn-impregnated zirconium oxide, exhibited somewhat complicated reduction behaviour. With regard to the reduction of zirconium oxide phase, the high temperature TPR peak (640°C) of pure zirconium oxide moved down to 585°C and the low temperature peak (420°C) was not shown well. A similar result was observed in 5Mn/Zr. In 5Mn/Zr-IM and 5Mn/Zr, the amount of hydrogen consumption for the high temperature peak of zirconium oxide was 2.9×10^{-5} and 3.1×10^{-5} mol/g cat, respectively. Figure 4 shows the IR spectra of hydroxyl groups on the surface of zirconium oxide. Two absorption bands at 3775 and 3685 cm^{-1} have been assigned to the terminal and bridged groups, respectively (*17*). The addition of small amounts of manganese leads to a decrease of the 3775 cm^{-1} band compared with the 3685 cm^{-1} band. These changes of surface hydroxyl groups are considered to be responsible for the disappearance of the low temperature peak of zirconium oxide in the TPR. Hydrogen consumption by the reduction of the manganese oxide phase produced one prominent peak at 185°C and two weak peaks as shoulders at 320°C and 455°C. The last two weak peaks correspond to the reduction of bulk manganese oxide particles. The low temperature peak located at 185°C may be ascribed to the presence of highly dispersed manganese oxide on the zirconium oxide surface, whose properties must be quite different from those of the bulk manganese oxide. The TPR pattern of 5Mn/Zr, the coprecipitated oxide, was similar to that of 5Mn/Zr-IM, except that the two peaks for the bulk manganese oxide (320°C, 455°C) were not well resolved. The absence of the bulk manganese oxide phase in 5Mn/Zr is in accordance with the previous results observed in the X-ray diffraction analysis (A′ in Fig. 2).

Similar TPR results of the presence of one prominent peak in the TPR profiles were also observed for V_2O_5 supported on other oxides such as silica, alumina, MgO, and TiO_2 (*18, 19*). Generally, the bulk phase of V_2O_5 yielded three or four reduction peaks during the TPR measurement in the temperature range from 650 to 800°C (*20, 21*). However, single or double layers of V_2O_5 immobilized on the supports yielded only one prominent reduction peak, which was located at a temperature between 440 and 590°C depending on the type of support.

When the manganese content was increased to 20% in the mixed oxide (Fig. 3D), two well-resolved peaks for the bulk manganese oxide appeared. The presence of large particles of Mn_2O_3 and Mn_3O_4 had already been confirmed by the X-ray diffraction results in Fig. 2. Note that the reduction peak of the surface-dispersed manganese oxide moved to higher temperature when compared with the peak observed at 185°C for 5Mn/Zr. This is caused by the increase in the number of manganese oxide layers dispersed on the zirconium oxide surface. The same phenomena have been observed in the

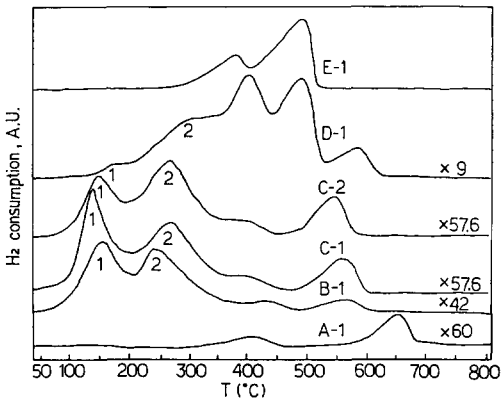

FIG. 5. Repeated TPR profiles of catalysts after TPR experiments followed by oxidation at 500°C. (A-1) Zr after the 1st TPR; (B-1) 5Mn/Zr-IM after the 1st TPR; (C-1) 5Mn/Zr after the 1st TPR; (C-2) 5Mn/Zr after the 2nd TPR; (D-1) 20Mn/Zr after the 1st TPR; (E-1) Mn after the 1st TPR.

case of V_2O_5 supported on silica; the reduction peak is increased from 510°C to 550°C with the increase in the V_2O_5 loading from 0.8% to 3.6% (*19*).

Figure 5 shows repeated TPR profiles for selected oxides after the first TPR is followed by an oxidation-TPR cycle. Except for pure zirconium and manganese oxide, the repeated reduction of Mn/Zr mixed oxides created a new TPR peak (peak 2 in Fig. 5) which was located at higher temperature than the TPR peak for the surface-dispersed manganese oxide (peak 1). Moreover, when compared with the same peak after the first TPR in Fig. 3, peak 1 moved to lower temperature and its intensity was substantially decreased for all samples of Mn/Zr oxide. We suggest that the new peak 2 arises from a solid solution which is formed after the sample is heated up to 800°C during the first TPR experiment. Therefore, the first TPR peak in Fig. 3 is considered a mixture of unresolved peaks of the surface-dispersed manganese oxide and the solid solution. As the TPR experiment is repeated (C-1 and C-2), the peak intensity for the solid solution phase increases while that for the surface-dispersed manganese oxide decreases. The results also indicate that the solid solution is formed at the expense of the surface-dispersed manganese oxide layers.

Figure 6 directly supports the facilitation in the formation of the solid solution by the repeated TPR treatment. After the second TPR in Fig. 5, the sample was subjected to X-ray diffraction analysis, and the results show a remarkable shift of the diffraction lines when compared with those of pure zirconium oxide having tetragonal structure. These shifts confirm the presence of manganese oxide in the zirconium oxide lattice; that is, the formation of a solid solution (*22*). In addition to the peak shift, the broad zirconium oxide peaks before the first TPR became very sharp after the second TPR due to the sintering of zirconium oxide particles.

Reaction Tests

Table 3 shows activity and selectivity data for the CO hydrogenation reaction at atmospheric pressure. Pure zirconium oxide produced appreciable amounts of methanol and dimethyl ether when the reaction temperature was kept below 400°C, as was observed by the Ekerdt group (*6*). At temperatures above 400°C, the oxygenated products were disappeared and substituted for butenes, mainly 1-butene and isobutene. The forma-

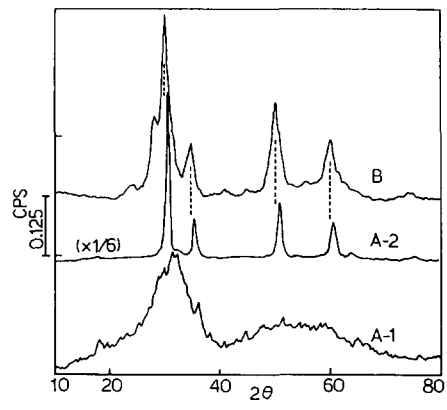

FIG. 6. X-ray diffraction patterns of catalysts. (A-1) 20Mn/Zr calcined at 500°C for 3 hr; (A-2) 20Mn/Zr after 2nd TPR; (B) tetragonal phase of zirconium oxide.

TABLE 3

Product Distribution in CO Hydrogenation

Catal.	Temp. (°C)	Selectivity (wt%)[a]								Rate × 10^1 mmole	Rate × 10^4 mmole
		CH_4	C_2H_4	C_2H_6	C_3H_6	C_4H_8	DME	CH_3OH	C_{5+}	g cat · h	m^2 · h
Mn-N	350	30.9	14.8	—	8.1	41.5	—	—	—	1.346	17.48
	400	15.4	10.0	—	5.6	47.2	—	—	21.9	3.159	41.03
	450	29.0	25.0	2.9	10.7	25.2	—	—	5.2	5.684	73.82
95Mn/Zr	300	72.0	13.8	—	14.2	—	—	—	—	0.355	2.22
	350	48.2	13.2	—	25.8	12.8	—	—	—	0.832	5.20
	400	34.6	17.1	—	9.7	30.5	—	—	8.1	2.089	13.06
	450	37.0	26.5	2.4	11.8	18.2	—	—	4.1	3.430	21.44
50Mn/Zr	300	65.9	17.3	—	16.7	—	—	—	—	0.369	0.25
	350	53.4	28.0	—	18.6	—	—	—	—	0.739	0.49
	400	34.5	22.8	1.6	12.1	22.7	—	—	6.3	1.736	1.16
	450	46.7	24.5	3.0	15.6	7.5	—	—	2.8	2.543	1.70
20Mn/Zr	300	68.5	14.1	—	17.4	—	—	—	—	0.429	0.23
	350	57.9	22.5	—	19.6	—	—	—	—	0.672	0.35
	400	41.2	16.5	1.1	12.7	26.0	—	—	3.6	1.993	1.03
5Mn/Zr	300	62.2	6.9	—	30.9	—	—	—	—	0.384	0.40
	350	54.2	24.7	—	21.1	—	—	—	—	0.961	1.01
	400	36.5	16.0	—	12.1	35.4	—	—	—	2.120	2.23
	450	37.0	19.7	2.8	14.8	25.7	—	—	—	4.227	4.45
Zr	300	28.0	2.5	—	—	—	36.7	32.8	—	0.673	1.03
	350	32.5	4.6	—	—	17.4	14.5	31.0	—	0.971	1.49
	400	35.1	8.0	1.2	4.7	51.0	—	—	—	1.364	2.10
	450	37.9	12.3	4.1	9.6	36.1	—	—	—	2.632	4.05
5Mn/Zr-IM	300	72.5	13.8	—	13.7	—	—	—	—	0.521	0.84
	350	53.4	19.7	—	15.9	11.0	—	—	—	1.029	1.66
	400	18.7	16.0	1.2	12.5	37.4	—	—	14.2	3.240	5.23
	450	27.3	28.1	6.5	18.6	15.2	—	—	4.3	6.182	9.97

[a] Product distribution is exclusive of water and carbon dioxide.

tion of butenes became maximum at 400°C, and its selectivity reached 50%. At this temperature the portion of isobutene among butenes was about 80%. Maruya and co-workers (*4*, *5*) reported that zirconium oxide selectively produced isobutene, and the selectivity of isobutene was about 70% at 400°C. The difference in the selectivity value is probably due to the difference in the reaction system; we used the once-through fixed-bed reactor while Maruya used a batch recirculating reaction system.

Pure manganese oxide was found to be as active and selective as zirconium oxide for the production of isobutene. When the catalytic activity was based on the surface area, manganese oxide exhibited one order of magnitude higher activity than zirconium oxide. Compared with zirconium oxide, pure manganese oxide did not produce any oxygenated products even at temperatures below 400°C. At the reaction temperature of 400°C, the isobutene selectivity was as high as that of zirconium oxide and the production of methane was suppressed. However, the decrease in the production of methane resulted in a corresponding increase in the production of additional hydrocarbons with carbon numbers higher than C_5.

In the case of Mn–Zr mixed oxides, the

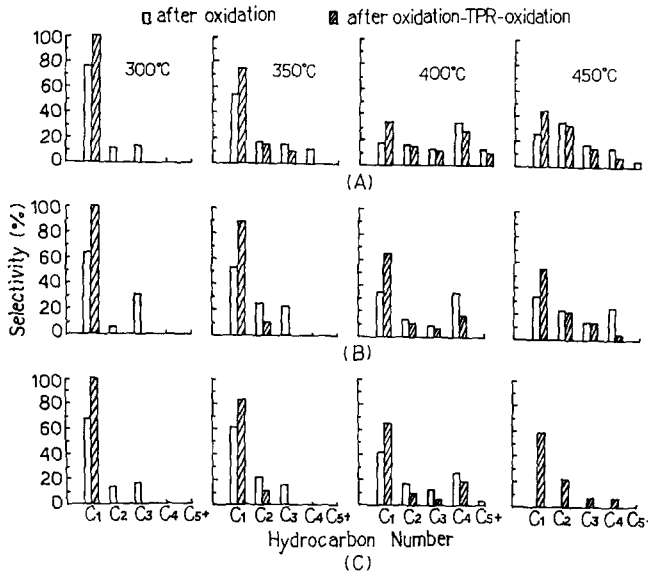

FIG. 7. Product distribution of fresh and TPR-treated catalysts at various reaction temperatures. (A) 5Mn/Zr-IM, (B) 5Mn/Zr, (C) 20Mn/Zr.

introduction of a small amount of Mn into Zr effectively suppressed the formation of oxygenated products. Therefore, we assume that the incorporation of Mn removes a catalytic site on pure zirconium oxide which is responsible for the production of alcohol. According to studies of zirconium oxide by the Ekerdt group (*6–10*), it is known that surface hydroxyl groups are needed for the formation of alcohol on zirconium oxide. Our TPR and IR results have shown that the doped Mn preferentially removes terminal hydroxyl groups from zirconium oxide. Therefore, it can be concluded that the terminal hydroxyl groups are responsible for the formation of oxygenated compounds. When the manganese content is low, as in the case of 5Mn/Zr, hydrocarbons higher than C_5 are not formed. From the XRD and TPR results of 5Mn/Zr, it is known that a part of Mn is incorporated into the bulk phase of zirconium oxide by forming a solid solution and that a part of Mn forms a highly dispersed layer on the zirconium oxide surface. Therefore, it can be established that manganese oxide, which is dispersed as thin layers, has a tendency to prohibit the formation of long chain hydrocarbons higher than C_5. With increased Mn content, however, there were corresponding increases in the productions of long chain hydrocarbons (C_{5+}). It is believed that the presence of large particles of bulk phase Mn oxide in the catalyst sample causes the increased yield of the long chain hydrocarbons. When catalytic activity is based on the catalyst surface area, a substantial decrease in the catalytic activity is observed when Mn content is in the region of 20–50%, where it is easy to form the Mn–Zr solid solution. Therefore, we suggest that the formation of the solid solution is responsible for the increased production of methane. To support the suggestion, product distributions after oxidation and TPR experiments were compared in Fig. 7. After the TPR experiment all the catalysts showed an increased selectivity to methane production. This can be related to the observed results of the increase in the formation of the solid solution after re-

peated oxidation–TPR cycles. Therefore, our future research will be directed to finding a way to increase the surface area of manganese oxide without forming a solid solution.

CONCLUSIONS

The precipitated Mn–Zr mixed oxide is composed of a heterogeneous mixture of large particles of manganese oxide and small particles of zirconium oxide. Thus, the addition of Mn reduces the probability of contact among zirconium oxide particles and retards crystallite growth of zirconium oxide. After calcination at 500°C, a part of manganese oxide forms a solid solution with zirconium oxide and a part of manganese oxide is dispersed on the surface of zirconium oxide. The formation of a solid solution was accelerated by increasing the treatment temperature. Mn dispersed on the surface of zirconium oxide effectively blocked a catalytic site on zirconium oxide which is responsible for the formation of oxygenated products. The selectivity pattern in the CO hydrogenation is dependent on the type of Mn present in the mixed oxide. The bulk manganese oxide exhibits a similar selectivity pattern to that of pure zirconium oxide, except the oxygenated products are substituted for hydrocarbons higher than C_5. The surface-dispersed manganese oxide layer produces only hydrocarbons up to C_4 with similar high selectivity toward butenes as pure zirconium oxide, and the solid solution enhances the production of methane.

ACKNOWLEDGMENT

We are grateful to the Korean Science Foundation for their support of the present work.

REFERENCES

1. Denise, B., Sneeden, R. P. A., Beguin, B., and Cherifi, O., *Appl. Catal.* **30,** 353 (1987).
2. Denise, B,. and Sneeden, R. P. A., *Appl. Catal.* **28,** 235 (1986).
3. Ichikawa, M., *J. Chem. Soc. Chem. Commun.*, 566 (1978).
4. Maruya, K., Maehashi, T., Haraoka, T., Narui, S., Asakawa, Y., Domen, K., and Onishi, T., *Bull. Chem. Soc. Jpn.* **61,** 667 (1988).
5. Maehashi, T., Maruya, K., Domen, K., Aika, K., and Onishi, T., *Chem. Lett.*, 747 (1984).
6. He, M.-Y., White, J. M., and Ekerdt, J. G., *J. Mol. Catal.* **30,** 415 (1985).
7. He, M.-Y., and Ekerdt, J. G., *J. Catal.* **90,** 17 (1984).
8. Tseng, S. C., Jackson, N. B., and Ekerdt, J. G., *J. Catal.* **109,** 284 (1988).
9. Jackson, N. B., and Ekerdt, J. G., *J. Catal.* **101,** 90 (1986).
10. Silver, R. G., Hou, C. J., and Ekerdt, J. G., *J. Catal.* **118,** 400 (1989).
11. Roper, M., Keim, W., Seibring, J., and Kolle-Gorgen, G., European Patent 208 102 (1987).
12. Keim, W., and Falter, W., *Catal. Lett.* **3,** 59 (1989).
13. Subbarao, E. C., *in* "Advances in Ceramics" (A. H. Heuer and L. W. Hobbs, Eds.), Vol. 3, p. 1. Columbus, Ohio, 1981.
14. Thompson, M. A., Young, D. R., and McCartney, E. R., *J. Am. Ceram. Soc.* **56,** 648 (1973).
15. Livage, J., Doi, K., and Mazieres, C., *J. Am. Ceram. Soc.* **51,** 349 (1968).
16. Tret'yakov, N. E., and Filimonov, V. N., *Kinet. Katal.* **13,** 815 (1972).
17. Yamaguchi, T., Nakano, Y., and Tanabe, K., *Bull.Chem. Soc. Jpn.* **51,** 2482 (1978).
18. Kijenski, J., Baiker, A., Glinski, M., Dollenmeier, P., and Wokaun, A., *J. Catal.* **101,** 1 (1986).
19. Kip, B. J., Smeets, P. A. T., van Wolput, J. H. M. C., Zandbergen, H. W., van Grondelle, J., and Prins, R., *Appl. Catal.* **33,** 157 (1987).
20. Bosch, H., Kip, B. J., van Ommen, J. G., and Gellings, P. J., *J. Chem. Soc. Faraday Trans. 1* **80,** 2479 (1984).
21. Baiker, A., and Monti, D., *J. Catal.* **91,** 361 (1985).
22. Jensen, K. B., and Massoth, F. E., *J. Catal.* **92,** 98 (1985).